JOURNAL OF CATALYSIS **163,** 409–417 (1996)
ARTICLE NO. 0342

Kinetics of Selective Catalytic Reduction of Nitric Oxide by Ammonia over Vanadia/Titania

J. A. Dumesic,* N.-Y. Topsøe,† H. Topsøe,† Y. Chen,† and T. Slabiak†

*Department of Chemical Engineering, University of Wisconsin, Madison, Wisconsin 53706; and †Haldor Topsøe Research Laboratories, DK-2800, Lyngby, Denmark

Received January 29, 1996; revised April 29, 1996; accepted May 1, 1996

A kinetic model based on a previously proposed reaction scheme was used to describe reaction kinetics measurements for the selective catalytic reduction of nitric oxide by ammonia over a 6 wt% vanadia/titania catalyst in the presence of oxygen (2 mol%) at nitric oxide and ammonia concentrations from 100 to 500 ppm and at temperatures of 523 and 573 K. This reaction scheme involves adsorption of ammonia on Brønsted acid sites (V^{5+}–OH), followed by activation of ammonia via reaction with redox sites (V=O). This activated form of ammonia reacts with gaseous or weakly adsorbed NO, producing N_2 and H_2O, and leading to partial reduction of the catalyst. The V^{4+}–OH species formed by the selective catalytic reduction (SCR) reaction combine to form water, and the catalytic cycle is completed by reaction of the reduced sites with O_2. Water adsorbs competitively with ammonia on acid sites. This reaction scheme can be used to describe the kinetics of the SCR reaction under laboratory as well as under industrially relevant reaction conditions.

INTRODUCTION

The selective catalytic reduction (SCR) of nitric oxide by ammonia over vanadia/titania catalysts is an effective process for NO_x emissions control from stationary sources (e.g., (1)). One of the major issues for the industrial utilization of this technology is to achieve high levels of nitric oxide conversion and to minimize emissions of unreacted ammonia (ammonia slip). It is of importance to understand the factors that control the reaction kinetics over a wide range of reaction conditions, since simplified kinetic treatments may have severe limitations in situations where removal of compounds to the ppm level is required, e.g., ultrapurification or zero emission devices (2–6).

Recent studies have shown that the kinetic rate expression for the SCR reaction over vanadia/titania catalysts is complex, such that the observed reaction orders with respect to nitric oxide and ammonia depend on reaction conditions (e.g., (2, 7–9)). In addition, results from recent FTIR spectroscopic studies have provided important information about the nature and coverages of surface species on vanadia/titania catalysts under SCR reaction conditions (e.g., (10–13)). In the present paper, we report reaction kinetics data for the selective reduction of nitric oxide by ammonia, collected on catalyst powders to minimize possible effects of transport limitations. These kinetic data were obtained for the same vanadia/titania catalysts that were employed for *in situ* Fourier transform infrared (FTIR) spectroscopic studies of the SCR reaction (12, 13). This selection of catalyst enables one to use the information obtained in these previous spectroscopic studies to provide a more quantitative description of the performance of vanadia/titania catalysts under various reaction conditions.

EXPERIMENTAL AND RESULTS

The catalysts used in this study are the same as those used previously in our *in situ* FTIR studies (12, 13). These materials were prepared by impregnating the titania support (anatase form, surface area of 90 m^2/g) with an oxalic acid solution of ammonium metavanadate, followed by drying at 375 K and calcination at 675 K for 1 h.

Reaction kinetics measurements were carried out at 523 and 573 K under ambient pressure in a glass-lined stainless steel reactor. Sieved fractions (75 to 150 μm) of the sample consisting of small amounts of catalyst diluted in an inactive titania matrix were loaded into a reactor (length of catalyst bed equal to 30 mm) that was subsequently attached to an experimental apparatus that has been described previously (14).

The reactant gas with the desired concentrations of NO, NH_3, and O_2 was prepared in a gas manifold equipped with electronic mass flow meters (Brooks) and monitored by a Balzers QMG 420 quadrupole mass spectrometer equipped with a heated, continuous gas inlet. The mass spectrometer data were quantitatively analyzed using the fragmentation patterns determined experimentally from calibration gases.

The catalyst samples which were loaded in the reactor were treated for 16 h at 673 K in 8 mol% O_2/Ar at a flow rate of 100 ml(NTP)/min. After cooling to the desired reaction temperature, the reactor was by-passed and the gas was exchanged with the reactant gas mixture at a flow rate

0021-9517/96 $18.00

of 200 ml(NTP)/min. Upon stabilization of the intensities measured with the mass spectrometer, the gas mixture was passed through the reactor and the nitric oxide conversions were determined.

Table 1 presents nitric oxide conversions (X_{NO} exp) measured over the 6 wt% V_2O_5/TiO_2 catalyst at 523 and 573 K for various NO and NH_3 inlet concentrations from 100 to 500 ppm in 2 mol% O_2 at the flow rate of 200 ml(NTP)/min. Most of these data were collected using 2.5 mg of the 6% V_2O_5/TiO_2 catalyst mixed with 123 mg of TiO_2. Additional experiments were conducted at lower conversions by using 1.2 mg of the 6% V_2O_5/TiO_2 catalyst mixed with 123 mg of TiO_2. Experimental ammonia conversions were also measured; however, these values are less reliable than X_{NO}, since long times were required to reach stable readings in the mass spectrometer due to adsorption of ammonia on various surfaces in the measuring chamber.

TABLE 1

Nitric Oxide Conversions (X_{NO}) over 6% V_2O_5/TiO_2 at 523 and 573 K for Various NO and NH_3 Inlet Concentrations in 2 mol% O_2 at a Flow Rate of 200 ml(NTP)/min

Temp. (K)	Cat. wt (mg)	NH_3 (ppm)	NO (ppm)	NH_3/NO	X_{NO} exp (%)	X_{NO} fit (%)
523	2.5	100	504	0.20	18	18
523	2.5	103	404	0.25	19	20
523	2.5	103	404	0.25	19	20
523	2.5	192	504	0.38	20	19
523	2.5	195	505	0.39	20	19
523	2.5	196	502	0.39	19	19
523	2.5	93	204	0.46	24	24
523	2.5	95	204	0.47	24	24
523	2.5	399	504	0.79	20	19
523	2.5	403	504	0.80	20	19
523	2.5	103	104	0.99	29	28
523	2.5	503	503	1.00	20	20
523	2.5	104	104	1.00	30	28
523	2.5	535	503	1.06	20	20
573	2.5	195	505	0.39	37	35
573	2.5	196	502	0.39	35	35
573	2.5	93	204	0.46	39	39
573	2.5	95	204	0.47	39	40
573	2.5	399	504	0.79	40	38
573	2.5	403	504	0.80	39	38
573	2.5	103	104	0.99	46	44
573	2.5	503	503	1.00	40	38
573	2.5	104	104	1.00	46	44
573	2.5	535	503	1.06	40	38
523	1.2	283	500	0.57	5	10
523	1.2	515	504	1.02	7	10
523	1.2	117	105	1.11	10	14
523	1.2	117	104	1.13	13	14
523	1.2	130	104	1.25	11	14
573	1.2	283	500	0.57	13	20
573	1.2	515	504	1.02	16	20
573	1.2	117	105	1.11	20	24
573	1.2	117	104	1.13	20	24
573	1.2	130	104	1.25	20	24

Analyses of reaction kinetics data were conducted in this study using general regression software (GREG) and a nonlinear equation solver (NNES) provided by W. E. Stewart and R. Bain (University of Wisconsin). The procedures used in these analyses are described elsewhere (6).

DISCUSSION

Survey of Catalytic Cycles Proposed in the Literature

Takagi *et al.* (15, 16) proposed a Langmuir–Hinshelwood reaction between adsorbed NO_2 and adsorbed NH_4^+. However, Inomata *et al.* (17) did not observe oxidation of NO to NO_2 by O_2 in dilute gas mixtures (1000 ppm NO in 1 mol% O_2) typical of industrial reaction conditions. Furthermore, Topsøe (11, 18) did not detect NO_2 on the catalyst surface under SCR conditions. Odriozola *et al.* (19) considered vanadia/titania as a bifunctional catalyst and suggested a Langmuir–Hinshelwood reaction between NO adsorbed on TiO_2 and NH_3 adsorbed on V^{5+}. Spectroscopic studies have revealed, however, that significant amounts of adsorbed NO are not present during the SCR reaction (11, 18, 20, 21). Therefore, reaction kinetics measurements showing that the SCR reaction order with respect to NO is less than unity (e.g., (2, 7, 8)) cannot be explained by the blocking of surface sites by adsorbed NO species. Bosch *et al.* (22) proposed a redox mechanism, which is supported by Janssen *et al.* (23), where V^{5+} is first reduced by NH_3 and is subsequently reoxidized by NO.

Inomata *et al.* (17) suggested that NO reacts with NH_3 adsorbed on dual sites comprised of V−OH and an adjacent V=O species which assists in the activation of NH_3. They found that the surface concentration of V=O was proportional to the rate of reaction between NH_3 and NO. A similar mechanism was suggested by Efstathiou and Fliatoura (9). Gasior *et al.* (21) proposed that V−OH was the active site. This suggestion has since been supported by several investigators (18, 24, 25). More recently, Ramis *et al.* (26) proposed an oxidation/reduction mechanism in which the reaction takes place between strongly adsorbed ammonia and gaseous or weakly adsorbed NO. Went *et al.* (27) have suggested that the SCR reaction over vanadia/titania occurs by reaction of adsorbed NO with an activated form of ammonia, e.g., adsorbed NH_2 species.

In addition to the findings that adsorbed ammonia species are predominant on vanadia/titania catalysts under SCR reaction conditions (11, 14, 15, 17, 28), *in situ* IR measurements (11, 28) revealed that ammonia is adsorbed on both Brønsted and Lewis acid sites under reaction conditions. Furthermore, ammonia adsorption was suggested (2, 13) to be equilibrated under typical SCR reaction conditions. As discussed above, significant amounts of adsorbed NO could not be detected on the catalyst surface under reaction conditions. The results of these spectroscopic studies and related

kinetic information were shown by Dumesic *et al.* (2) to be described by a catalytic cycle consisting of equilibrated ammonia adsorption, activation of the adsorbed ammonia, and subsequent reaction of the activated ammonia species with gaseous or weakly adsorbed NO. This mechanism described quantitatively the NO conversion data as well as the ammonia slip for the vanadia/titania catalyst system obtained under industrially relevant conditions.

To obtain more detailed mechanistic insight, Topsøe *et al.* (12) recently employed *in situ* FTIR and on-line mass spectrometry to study the surface species and the gaseous reaction products when preadsorbed ammonia on vanadia/titania catalysts was exposed to either $NO + O_2$, NO, or O_2 under temperature-programmed reaction conditions. Lewis and Brønsted acid sites are present on the surfaces of these catalysts, with the Brønsted acid sites being associated with V^{5+}–OH species. Ammonia preadsorbed on vanadia/titania reacted in flowing $NO + O_2$ or NO to form N_2. This reaction of preadsorbed ammonia with NO over vanadia/titania produced new V–OH bands at higher frequencies, related to some new reduced vanadia species. These vanadyl bands on oxidized vanadia/titania catalysts are converted to bands at lower frequencies upon ammonia adsorption. The original vanadyl bands characteristic of the oxidized catalyst are restored upon heating samples containing preadsorbed ammonia in flowing $NO + O_2$, while this process was slower in flowing NO. These results suggest that the surface becomes reduced upon reaction of preadsorbed ammonia with NO, and the catalyst is reoxidized primarily by reaction with O_2.

In a parallel study, Topsøe *et al.* (13) used *in situ* FTIR and on-line mass spectrometry to monitor the surface and catalytic properties of vanadia/titania under SCR reaction conditions. The adsorption of ammonia was shown to be an equilibrated step during typical SCR reaction conditions. The SCR reaction rate was observed to depend on the concentrations of surface vanadyl species and ammonia adsorbed on Brønsted acid sites, suggesting that vanadyl species react with ammonia on Brønsted acid sites to form a surface species that subsequently reacts with nitric oxide. This ammonia activation step was proposed to take place by complete or partial H-transfer from ammonium ions to surface vanadyl species. Again, observable amounts of adsorbed nitric oxide species were not revealed under reaction conditions. In agreement with the transient studies (12), it was found that the SCR reaction leads to the production of new V–OH species associated with reduced vanadium cations, and these species are present in significant concentrations on the catalyst under SCR reaction conditions.

Based on the surface chemical insight provided by the aforementioned spectroscopic studies, the following general conclusions regarding the catalytic cycle for the SCR reaction were proposed (10–13, 20): (i) adsorbed ammonia species are the most abundant surface species under reaction conditions, (ii) Brønsted acid sites appear to be active sites for the SCR reaction, (iii) the adsorption of ammonia on these sites appears to be an equilibrated process in the SCR reaction, (iv) the activation of adsorbed ammonia by reaction with surface vanadyl species appears to be necessary prior to reaction with NO, (v) significant amounts of adsorbed NO are not present on the catalyst surface under reaction conditions, (vi) selective catalytic reduction of NO involves reaction of gaseous or weakly adsorbed NO with the activated ammonia species, producing N_2 and H_2O, and leading to partial reduction of the catalyst, and (vii) the catalytic cycle is completed by reaction of the reduced sites with O_2.

Analysis of Experimental Results

The spectroscopic and chemical information summarized in the previous section has been used to formulate a catalytic cycle for the SCR reaction (i.e., $NO + NH_3 + \frac{1}{4}O_2 \rightarrow N_2 + \frac{3}{2}H_2O$) in terms of acid and redox components. This cycle is shown as Scheme 1.

Step 1 is equilibrated under typical SCR reaction conditions (9, 14). Step 2 is the ammonia activation step, and it is not necessarily equilibrated. Gaseous or weakly adsorbed, NO reacts in step 3 with surface species $V{-}ONH_3{-}V^{4+}{-}OH$ to form N_2 and H_2O. This step is probably not an elementary reaction, since the reverse of this step is very unlikely to take place as written. Accordingly, we write step 3 as an irreversible process, assuming that the reaction between NO and species $V{-}ONH_3{-}V^{4+}{-}OH$ involves the initial formation and/or rearrangement of a highly reactive surface complex. The removal of surface hydroxyl groups to form water is described in step 4. In general, this may be a reversible step, especially at high water concentrations. At industrial SCR reaction conditions, the catalyst surface is essentially fully oxidized. Accordingly, the surface concentration of reduced sites, V^{3+}, should be sufficiently low to make step 4 irreversible. Step 5 represents reoxidation of the catalyst by O_2. This step should be kinetically insignificant, provided that it takes place at a rate sufficient to

(1) $$NH_3 + V^{5+}{-}OH \rightleftarrows V{-}ONH_4$$

(2) $$V{-}ONH_4 + V{=}O \rightleftarrows V{-}ONH_3{-}V^{4+}{-}OH$$

(3) $$NO + V{-}ONH_3{-}V^{4+}{-}OH \rightarrow N_2 + H_2O + V^{5+}{-}OH + V^{4+}{-}OH$$

(4) $$2V^{4+}{-}OH \rightleftarrows H_2O + V^{3+} + V{=}O$$

(5) $$O_2 + 2V^{3+} \rightarrow 2V{=}O$$

(6) $$H_2O + V^{5+}{-}OH \rightleftarrows V^{5+}{-}OH_3O$$

SCHEME 1

maintain the catalyst in a fully oxidized state. Finally, step 6 involves the competitive adsorption of water on acid sites, and this step is equilibrated under steady state SCR reaction conditions, since the species $V^{5+}{-}OH_3O$ only appears in this step. It should be noted that formal valence states shown in Scheme 1 are provided for convenience to account for reduction of the catalyst during the catalytic cycle. It is possible, for example, that a V^{3+} center may react with a neighboring V^{5+} cation to give two V^{4+} species; however, this possible process is kinetically insignificant for the SCR reaction in the presence of oxygen.

In general, Scheme 1 involves 11 rate constants (all steps are reversible with the exception of step 3), giving rise to 22 kinetic constants (i.e., preexponential factors and activation energies). Clearly, our kinetic data are not sufficient to allow estimates for all of these parameters, and assumptions must be made. Most importantly, we assume reasonable values for all preexponential factors based on transition state theory (6). These values were not adjusted further, with the exception of the forward preexponential factor for step 3. Since step 1 is an equilibrated process, it is only necessary to constrain the difference between the forward and reverse activation energies to be equal to the heat of adsorption. This heat has been estimated elsewhere (9, 14) to be approximately equal to 20 kcal/mol for high loadings of vanadia on titania, and this value was not adjusted further in our analyses. Since our reaction kinetics data were collected at low water concentrations, we can assume that step 4 is irreversible and step 6 is kinetically insignificant. The rate of O_2 desorption is expected to be negligible at the low temperatures of the present study, and step 5 can be assumed to be irreversible. Finally, we assume that the surface concentration of V=O sites is 10% of the surface concentration of V^{5+}–OH acid sites, since infrared spectroscopic results indicate that the predominant surface species under SCR reaction conditions is ammonia adsorbed on acid sites. This assumption is arbitrary, and different values can be used for the concentration of V=O sites, provided that the preexponential factors are adjusted accordingly. The concentration of V^{5+}–OH acid sites was assumed to be equal to 10^{15} cm^{-2}.

In view of the above assumptions, the reaction kinetics data were fitted using the following five adjustable parameters: A_3, E_2, E_{-2}, E_3, and E_4, where A_i, A_{-i}, E_i, and E_{-i} are the forward and reverse preexponential factors (A) and activation energies (E) for step i. The reactor was assumed to operate as a plug-flow reactor, and the adjustment of parameters was accomplished by an optimization procedure that minimized the sum of the squares of the differences between the experimental and predicted nitric oxide concentrations in the reactor effluent. The kinetic parameters resulting from this analysis are listed in Table 2.

The nitric oxide conversions predicted by Scheme 1 with the kinetic parameters of Table 2 are compared with the experimental data in Table 1. The agreement between the predicted and experimental values is very good. Importantly, the predicted values show the proper trend with inlet NH_3/NO ratio, as shown in Fig. 1. This figure presents the experimental values of the nitric oxide conversion versus NH_3/NO ratio over 2.5 mg of catalyst at 523 and 573 K at a constant NO concentration of about 500 ppm (circles) and also at a constant NH_3 concentration of about 100 ppm (squares). The predictions of Scheme 1 with the kinetic parameters of Table 2 are shown by the solid lines in Fig. 1. It can be seen that these predictions reproduce well the observed variations in nitric oxide conversion versus NH_3/NO

TABLE 2

Kinetic Parameters for Scheme 1 That Describe the Kinetic Data of the Present Study

Step	A_i[a]	E_i (kcal/mol)	A_{-i}[a]	E_{-i} (kcal/mol)
1	8×10^6	0	1×10^{13}	20
2	1×10^{11}	21.6 ± 2.2	1×10^{11}	32.1 ± 5.3
3	$3.6 \pm 0.1 \times 10^4$	5.5 ± 0.1	—	—
4	1×10^{11}	26.3 ± 0.6	—	—
5	8×10^2	0	—	—
6	—	—	—	—

[a] Units of sec^{-1} for surface reactions and sec^{-1} atm^{-1} for reactions involving gaseous (or weakly adsorbed) species.

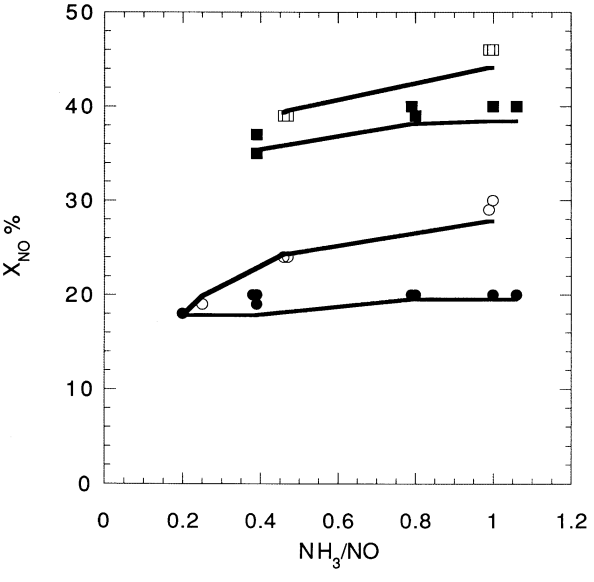

FIG. 1. Nitric oxide conversion (X_{NO}) versus inlet NH_3/NO ratio over 2.5 mg of 6% V_2O_5/TiO_2 catalyst for inlet NO concentrations of approximately 500 ppm at 523 K (●) and 573 K (■) and for inlet NH_3 concentrations of approximately 100 ppm at 523 K (○) and 573 K (□). Results of simulations using Scheme 1 and the kinetic parameters of Table 2 are shown as solid lines. Experimental and simulated nitric oxide conversions are reported in more detail in Table 1.

ratio at constant NO concentration, at constant NH_3 concentration, and at two different temperatures.

Under the reaction conditions of the present study containing 2 mol% O_2, the surface is essentially oxidized and the rate constant of step 5 is kinetically insignificant. However, the rate of the SCR reaction begins to decrease when the O_2 concentration decreases below approximately 1 mol% (e.g., see Ref. (1)). Therefore, we have set the value of the rate constant for step 5 to an appropriate value for which the kinetic model shows a decrease in the SCR rate at these lower O_2 concentrations.

Extrapolation to Industrially Relevant SCR Reaction Conditions

In a previous work (2), we reported SCR reaction kinetics data at two different space velocities over a 6% V_2O_5/TiO_2 catalyst at 623 K in 4 mol% O_2 and 5 mol% H_2O for an inlet NO concentration of 300 ppm and for NH_3/NO ratios from approximately 0.7 to 1.1. Under these experimental conditions, the SCR reaction is partially limited by internal mass transfer within the catalyst particles, and the effectiveness factor was shown to be near the value of 0.3.

A simplified three-step reaction sequence, shown below as Scheme 2, was found to describe satisfactorily the reaction kinetics data of the previous study, where M is an acid site onto which NH_3 adsorbs in step 1 and S is a site on which NH_3 is activated in step 2 for subsequent reaction with NO in step 3. Step 1 was assumed to be equilibrated, step 2 was allowed to be reversible, and step 3 was defined to be irreversible.

It is now interesting to test whether Scheme 1, with kinetic parameters similar to those in Table 2, can be used to describe the SCR kinetics data obtained under industrially relevant conditions. In order to account for the effects of water in steps 4 and 6, normal values of preexponential factors were assumed for step 6, with a heat of water adsorption equal to 16.5 kcal/mol (14); these values were not adjusted further. The reverse of step 4 is also assumed to be a nonactivated process, with a value of the preexponential factor that will be addressed further in the next section. Finally, for simplicity, the effectiveness factor is assumed to be equal to 0.2 at the higher space velocity and 0.3 at the lower space velocity.

Using the above assumptions, the reaction kinetics data of our previous study were fitted by a small adjustment of A_3. The reactor was assumed to operate as a plug-flow reactor. The kinetic parameters resulting from this analysis are listed in Table 3.

TABLE 3

Kinetic Parameters for Scheme 1 That Describe the Kinetic Data Collected under Industrially Relevant SCR Reaction Conditions (2)

Step	A_i[a]	E_i (kcal/mol)	A_{-i}[a]	E_{-i} (kcal/mol)
1	8×10^6	0	1×10^{13}	20
2	1×10^{11}	21.6	1×10^{11}	32.1
3	$1.3 \pm 0.1 \times 10^4$	5.5	—	—
4	1×10^{11}	26.3	1.9×10^4	0
5	8×10^2	0	—	—
6	8×10^7	0	1×10^{13}	16.5

[a] Units of sec^{-1} for surface reactions and $sec^{-1}\,atm^{-1}$ for reactions involving gaseous (or weakly adsorbed) species.

The nitric oxide conversions predicted by Scheme 1 with the kinetic parameters of Table 3 are compared with the experimental data in Fig. 2. This figure presents the experimental values of the nitric oxide conversion versus NH_3/NO ratio at space velocities of 181 l(NTP)/h/g (filled circles) and 58.7 l(NTP)/h/g (filled squares). The predicted values of the nitric oxide conversion are shown by the solid lines. It can be seen that the agreement between the predicted and experimental values is very good.

A more sensitive test of whether Scheme 1 can be used to describe the SCR kinetics data obtained under industrially

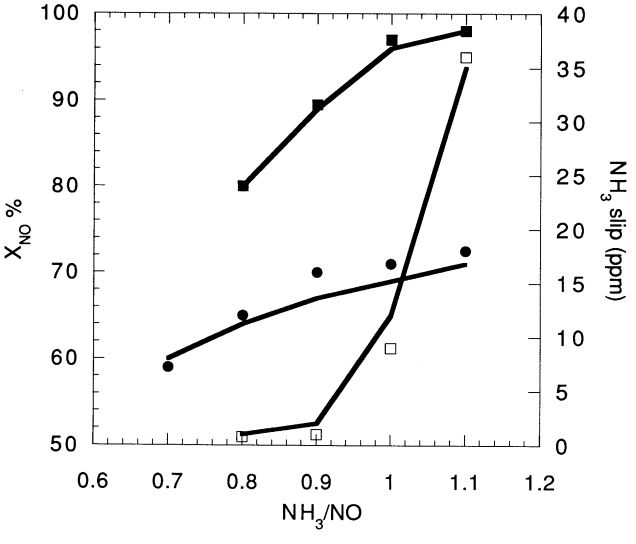

FIG. 2. Nitric oxide conversion (X_{NO}) and ammonia slip concentrations versus inlet NH_3/NO ratio in 4 mol% O_2 and 5 mol% H_2O at 623 K over 6% V_2O_5/TiO_2 catalyst for space velocities of 181 Nl/h/g (●) and 58.7 Nl/h/g (■, □). Filled symbols give nitric oxide conversions and open symbols give ammonia slip concentrations from Ref. 2. Results of simulations using Scheme 1 and the kinetic parameters of Table 3 are shown as solid lines.

(1) $$NH_3 + M \rightleftarrows NH_3M$$

(2) $$NH_3M + S \rightleftarrows M + NH_3S$$

(3) $$NO + NH_3S \rightarrow \text{Products}$$

SCHEME 2

relevant conditions is provided in Fig. 2 by comparing the effluent NH_3 concentration (i.e., the ammonia slip) from the reactor operating at the lower space velocity. The experimental values of the ammonia slip (open squares) are described well by the solid line representing the values predicted by Scheme 1 with the kinetic parameters of Table 3.

Analysis of Results from Lintz and Turek

Lintz and Turek (7) conducted an extensive study of the kinetics of nitric oxide reduction by ammonia over a vanadia/titania catalyst containing a high loading (20%) of vanadia. In particular, this study varied the concentrations of NO and NH_3 from approximately 100 to 1500 ppm, at water concentrations from 0 to 10 mol%, for an oxygen concentration of 4 mol%, and at temperatures of 523 and 623 K. We have taken the empirical rate expression reported by these authors to estimate the rate of the SCR reaction at 36 sets of experimental conditions covered in the study. Using these results we examine whether Scheme 1 can be used to describe their kinetic data with kinetic parameters similar to those given in Table 3. Moreover, since the experimental study by Lintz and Turek varied the concentration of water, it is possible to use these data to probe the reverse rate of step 4 and to test the validity of the equilibrium constant estimated above for adsorption of water in step 6.

Starting with the kinetic parameters of Table 2 and the equilibrium constant for step 6 given in Table 3, the SCR reaction rates estimated from the work of Lintz and Turek were fitted using the following six adjustable parameters: A_3, A_{-4}, E_2, E_{-2}, E_3, and E_4. The concentration of acid sites was assumed to be the same as for the high-loading vanadia/titania catalyst employed in the present study (i.e., 10^{15} cm^{-2}). The kinetic parameters resulting from this analysis are listed in Table 4.

Figure 3 presents a comparison of the experimental and predicted rates of nitric oxide reduction by ammonia over the range of NO, NH_3, and H_2O concentrations and temperatures studies by Lintz and Turek. The agreement between the experimental and predicted values is seen to be satisfactory at all conditions. In addition, it can be seen that the kinetic parameters given in Table 4 to fit the data of Lintz and Turek are very similar to the values given in Table 2 to describe the kinetic data of the present study and the values given in Table 3 to describe kinetic data obtained under industrially relevant SCR reaction conditions.

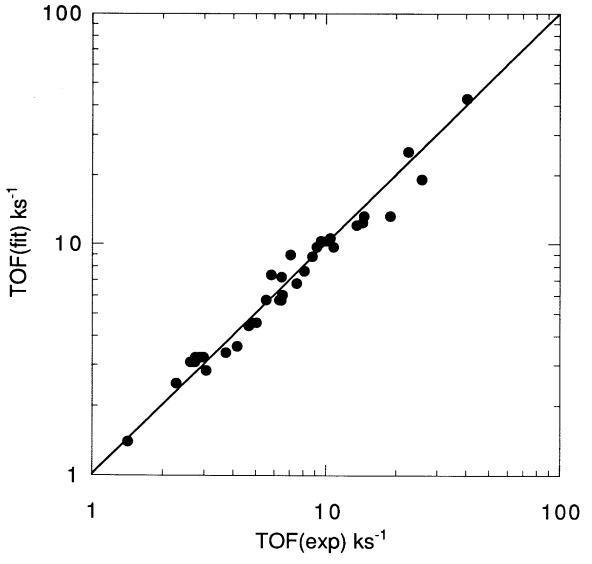

FIG. 3. Comparison of experimental SCR rates measured by Lintz and Turek (7) over a range of NO, NH_3, and H_2O concentrations and temperatures with SCR rates predicted by Scheme 1 with the kinetic parameters of Table 4.

Simulation of Temperature-Programmed Reaction Studies

In a previous study, we used temperature-programmed desorption (TPD) and temperature-programmed reaction (TPR) to study NH_3 desorption and the SCR reaction over a 6% V_2O_5/TiO_2 catalyst (14). As mentioned above, we have already used the TPD result from this previous study that the heat of ammonia adsorption on a 6% V_2O_5/TiO_2 catalyst is approximately 20 kcal/mol. However, it is also important to test whether Scheme 1 can be used to describe the TPR results using the kinetic parameters of Table 2 with the water adsorption parameters given in Table 3.

The TPR studies involved preadsorption of NH_3 on the 6% V_2O_5/TiO_2 catalyst, followed by heating in a flowing NO/Ar gas mixture (50 ml(NTP)/min, 3890 ppm NO) at a heating rate of 2 K/min. The concentration of NO in the reactor effluent passed through a minimum at ca. 430 K, corresponding to the maximum rate of the SCR reaction in this temperature-programmed experiment. In addition, the concentration of H_2O passed through a maximum at about 430 K, corresponding to the maximum rate of water production and desorption in this transient experiment.

TABLE 4

Kinetic Parameters for Scheme 1 That Describe the Kinetic Data Collected by Lintz and Turek (7)

Step	A_i[a]	E_i (kcal/mol)	A_{-i}[a]	E_{-i} (kcal/mol)
1	8×10^6	0	1×10^{13}	20
2	1×10^{11}	21.8 ± 2.2	1×10^{11}	31.6 ± 5.3
3	$6.2 \pm 0.1 \times 10^4$	5.5 ± 0.1	—	—
4	1×10^{11}	26.8 ± 0.6	$1.9 \pm 0.1 \times 10^4$	0
5	8×10^2	0	—	—
6	8×10^7	0	1×10^{13}	16.5

[a] Units of sec^{-1} for surface reactions and sec^{-1} atm^{-1} for reactions involving gaseous (or weakly adsorbed) species.

Simulations of these TPR experiments have been conducted by solving the differential equations that describe the changes in the gaseous pressures and the changes in the surface coverages by adsorbed species that accompany the heating of the catalyst in a flowing gas stream (6). The reactor was assumed to be well mixed in these simulations. Using Scheme 1 with the kinetic parameters of Table 2 and the water adsorption parameters of Table 3, the TPR simulations predict that the concentration of NO in the reactor effluent passes through a minimum at 450 K, while the concentration of H_2O passes through a maximum at 470 K. These temperatures are in good agreement with the experimental value of approximately 430 K. Thus, Scheme 1 is again shown to be able to capture the essential behavior of the SCR reaction under transient reaction conditions.

Approximate Rate Expression for the SCR Reaction

An important aspect of the experimental SCR kinetics data of the present study and the results of Lintz and Turek is that the reaction shows a fractional order (e.g., 0.7) with respect to the nitric oxide pressure. This behavior is described well by Scheme 1 and the kinetic parameters of Tables 2–4. In the present analyses, steps 1 and 6 are equilibrated, steps 3 and 5 are irreversible, step 2 is reversible but not necessarily equilibrated, and step 4 is irreversible in the absence of water and reversible in the presence of water.

It is not possible to derive an analytical rate expression that is valid over the wide range of reaction conditions explored in this paper, including laboratory reactor studies and measurements under industrially relevant SCR reaction conditions. Instead, it is necessary to solve simultaneously the appropriate equations that describe the reactor performance and the surface steady state relations for adsorbed species (6). However, it is possible to derive a quite simple rate expression that is valid for the specific case where the water concentration is sufficiently low that step 4 becomes irreversible. In particular, we assume that steps 1 and 6 are equilibrated, steps 3–5 are irreversible, and step 2 is reversible. Furthermore, we neglect the contribution of $V{-}ONH_3{-}V^{4+}{-}OH$ species in the site balance for the $V^{5+}{-}OH$ sites, since the surface concentration of $V{=}O$ sites is much smaller than the surface concentration of $V^{5+}{-}OH$ acid sites. Under these conditions, the following rate expression can be used to describe the rate of NO conversion during the SCR reaction,

$$\text{Rate} = \frac{\alpha^2}{\beta}[\gamma - (\gamma^2 + \beta S/\alpha)^{1/2}]^2$$

$$\alpha = \frac{k_2 k_3 P_{NO} K_1 P_{NH_3}}{(k_{-2} + k_3 P_{NO})(1 + K_6 P_{H_2O} + K_1 P_{NH_3}) + k_2 K_1 P_{NH_3}}$$

$$\beta = 16 k_4 k_5 P_{O_2}$$

$$\gamma = (2k_5 P_{O_2})^{1/2} + (k_4)^{1/2}$$

S = ratio of $V{=}O$ to $V^{5+}{-}OH$ sites on the clean, fully oxidized catalyst (assumed to be equal to 0.1 in the present study),

where k_i and k_{-i} are forward and reverse rate constants, K_i are equilibrium constants, and P_i are pressures (in atm). Substitution of the kinetics parameters from Tables 2–4 into these expressions gives the rate of NO consumption in units of molecules per acid site per second.

Dynamic Aspects of the Catalytic Cycle for the SCR Reaction

It is useful to express Scheme 1 as a catalytic cycle involving participation of acid sites ($V^{5+}{-}OH$) and redox sites ($V{=}O$). The surface chemical aspects of this catalytic cycle were described elsewhere (10, 13), based on insight provided by spectroscopic studies. It is now possible to use the results of the present study to address the dynamic aspects of this catalytic cycle.

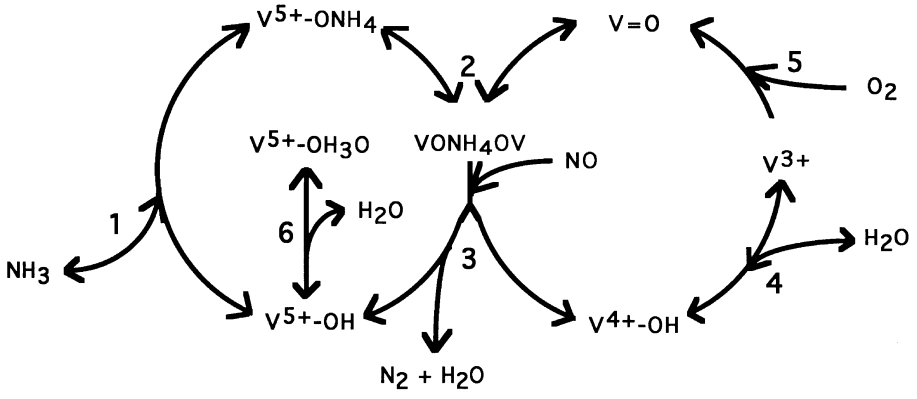

FIG. 4. Schematic representation of catalytic cycle for the SCR reaction over acid sites ($V^{5+}{-}OH$) and redox sites ($V{=}O$). The corresponding steps from Scheme 1 are indicated by the respective numbers on this diagram. Steps 1 and 6 involving the acid sites are equilibrated, steps 2 and 4 on the redox sites are reversible (but not generally equilibrated), and steps 3 and 5 on the redox sites are irreversible.

Figure 4 presents a schematic diagram of the catalytic cycle for the SCR reaction. Steps 1 and 6 take place over the acid sites (V^{5+}–OH), steps 3–5 occur over the redox sites (V=O), and step 2 provides coupling between the two types of sites. Steps 1 and 6 are equilibrated over the acid sites, while the steps that occur over the redox sites are either irreversible (steps 3 and 5) or reversible (step 4), but they are not generally equilibrated. In addition, the process that couples the functions of the two sites (step 2) is reversible but not equilibrated. Thus, the surface coverages on the acid sites are controlled by surface thermodynamics (e.g., the equilibrium constants of steps 1 and 6), while the surface coverages on the redox sites are controlled by surface dynamics (e.g., the rate constants for steps 2–5). In this latter respect, it is not appropriate to define a rate-determining step on the redox sites.

The results from the kinetic simulations of the present study suggest that no single surface species is most abundant on the catalyst over the wide range of SCR reaction conditions explored. In particular, the surfaces coverages on the acid sites by V–ONH_4 and V^{5+}–OH_3O become significant at high partial pressures of the respective gaseous species. Moreover, the surface coverages on the redox sites by V–ONH_3–V^{4+}–OH and V^{4+}–OH appear to be significant under all reaction conditions examined in this study. The only surface coverage that is low under the conditions of this study, involving gaseous O_2 concentrations higher than 1 mol%, is V^{3+} associated with the redox sites.

CONCLUSIONS

The present study shows that the recently proposed catalytic cycle (10–13) describes quantitatively the kinetics of the selective catalytic reduction of nitric oxide by ammonia over vanadia/titania catalysts under a wide range of reaction conditions. The catalytic cycle involves adsorption of ammonia on acid sites (V^{5+}–OH), activation of adsorbed ammonia by interaction with redox sites (V=O), reaction of activated ammonia with gaseous, or weakly adsorbed nitric oxide, recombination of surface hydroxyl groups (V^{4+}–OH) to form water, and reoxidation of reduced vanadium cations (V^{3+}) by O_2. Water competes with ammonia for adsorption on acid sites (V^{5+}–OH). The adsorption of ammonia on acid sites (V^{5+}–OH) is an equilibrated process, whereas the activation of adsorbed ammonia by reaction with redox sites (V=O) is reversible but not necessarily equilibrated. The recombination of surface hydroxyl groups (V^{4+}–OH) to form water is irreversible at low water concentrations, but it becomes reversible at higher water concentrations. Reaction of nitric oxide with activated ammonia on the surface and catalyst reoxidation by O_2 are irreversible processes.

Use of the kinetic parameters listed in Table 2 with Scheme 1 gives a good description of the SCR kinetics data of the present study collected over a 6% V_2O_5/TiO_2 catalyst in a laboratory reactor. The kinetic parameters listed in Table 3 can be used to describe the nitric oxide conversion and ammonia slip data collected over a 6% V_2O_5/TiO_2 catalyst under industrially relevant SCR reaction conditions. The SCR reaction kinetics data collected by Lintz and Turek on high loadings of vanadia on titania over a wide range of experimental conditions can be described using the kinetic parameters listed in Table 4. Finally, the TPD and TPR data collected over 6% V_2O_5/TiO_2 catalyst can be described with the kinetic parameters of Table 2 combined with the water adsorption parameters of Table 3. The kinetic parameters in Tables 2–4 have similar values, and we conclude that Scheme 1 provides an excellent description of the kinetics of the SCR reaction.

ACKNOWLEDGMENTS

We thank Eric Törnqvist, Bjerne Clausen, and Per Morsing (Haldor Topsøe A/S) for their valuable help throughout this project. In addition, we thank Randy Cortright (University of Wisconsin) for critical comments during analysis of the results. Finally, we thank W. E. Stewart and R. Bain for providing us with their computer software.

REFERENCES

1. Bosch, H., and Janssen, F. J. J. G., *Catal. Today* **2**, 369 (1988).
2. Dumesic, J. A., Topsøe, N.-Y., Slabiak, T., Morsing, P., Clausen, B. S., Törnqvist, E., and Topsøe, H., New Frontiers in Catalysis, "Proceedings of the 10th International Congress on Catalysis, Budapest" (L. Guczi, F. Solymosi, and P. Tetenyi, Eds.). Akadémiai Kiadó, Budapest, 1993. p. 1325.
3. Rostrup-Nielsen, J. R., Schoubye, P. S., Christiansen, L. J., and Nielsen, P. E., *Chem. Eng. Sci.* **49**, 3995 (1994).
4. Boudart, M., *Ind. Eng. Chem. Res.*, presented at Spring ACS Meeting, San Diego, 1994, Symposium on Catalytic Reaction Engineering for Environmentally Benign Processing.
5. Rostrup-Nielsen, J. R., "Elementary Reaction Steps in Heterogeneous Catalysis" (R. W. Joyner and R. A. van Santen, Eds.), pp. 441–460. Kluwer Academic, Dordrecht, 1993.
6. Dumesic, J. A., Rudd, D. F., Aparicio, L. M., Rekoske, J. E., and Trevino, A. A., "The Microkinetics of Heterogeneous Catalysis," Am. Chem. Soc. Washington, D.C., 1993.
7. Lintz, H. G., and Turek, T., *Appl. Catal. A* **85**, 13 (1992).
8. Robinson, W. R. A. M., van Ommen, J. G., Woldhuis, A., and Ross, J. R. H., 10th International Congress on Catalysis, Budapest (L. Guczi, F. Solymosi, and P. Tetenyi, Eds.). Akadémiai Kiadó, Budapest, 1993. p. 2673.
9. Efstathiou, A. M., and Fliatoura, K., *Appl. Catal. B* **6**, 35 (1995).
10. Topsøe, N.-Y., *Science* **265**, 1217 (1994).
11. Topsøe, N.-Y., and Topsøe, H., *Catal. Today* **2**, 77 (1991).
12. Topsøe, N.-Y., Topsøe, H., and Dumesic, J. A., *J. Catal.* **151**, 226 (1995).
13. Topsøe, N.-Y., Dumesic, J. A., and Topsøe, H., *J. Catal.* **151**, 241 (1995).
14. Srnak, T. Z., Dumesic, J. A., Clausen, B. S., Törnqvist, E., and Topsøe, N.-Y., *J. Catal.* **135**, 246 (1992).
15. Takagi, M., Kawai, T., Soma, M., Onishi, T., and Tamaru, K., *J. Catal.* **50**, 441 (1977).
16. Takagi-Kawai, M., Kawai, T., Soma, M., Onishi, T., and Tamaru, K., *J. Catal.* **57**, 528 (1979).

17. Inomata, M., Miyamoto, A., and Murakami, Y., *J. Catal.* **62**, 140 (1980).
18. Topsøe, N., *J. Catal.* **128**, 499 (1991).
19. Odriozola, J. A., Heinemann, H., Somorjai, G. A., Garcia de la Banda, J. F., and Pereira, P., *J. Catal.* **119**, 71 (1989).
20. Miyamoto, A., Yamazaki, Y., Hattori, T., Inomata, M. and Murakami, Y., *J. Catal.* **74**, 144 (1982).
21. Gasior, M., Haber, J., Machej, T., and Czeppe, T., *J. Mol. Catal.* **43**, 359 (1988).
22. Bosch, H., Janssen, F. J. J. G., Oldenziel, J., van den Kerkhof, F. M. G., van Ommen, J. G., and Ross, J. R. H., *Appl. Catal.* **25**, 239 (1986).
23. Janssen, F. J. J. G., van den Kerkhof, F. M. G., Bosch, H., and Ross, J. R. H., *J. Phys. Chem.* **91**, 5921 (1987).
24. Rajadhyaksha, R. A., and Knözinger, H., *Appl. Catal.* **51**, 81 (1989).
25. Chen, J. P., and Yang, R. T., *J. Catal.* **125**, 411 (1990).
26. Ramis, G., Busca, G., Lorenzelli, V., and Forzatti, P., *Appl. Catal.* **64**, 243 (1990).
27. Went, G. T., Leu, L.-J., Rosin, R. R., and Bell, A. T., *J.Catal.* **134**, 492 (1992).
28. Takagi, M., Kawai, T., Soma, M., Onishi, T., and Tamaru, K., *J. Phys. Chem.* **80**, 430 (1976).